Smart Structures and Systems, *Vol. 33*, *No. 4* (*2024*) *281-290*
https://doi.org/10.12989/sss.2024.33.4.281

Nonlinear dynamics of an adaptive energy harvester with magnetic interactions and magnetostrictive transduction

Pedro V. Savi and Marcelo A. Savi*

Universidade Federal do Rio de Janeiro, COPPE – Mechanical Engineering, Center for Nonlinear Mechanics, 21.941.972 - Rio de Janeiro – RJ – Brazil

(*Received July 21, 2023, Revised November 2, 2023, Accepted March 29, 2024*)

Abstract. This work investigates the mechanical energy harvesting from smart and adaptive devices using magnetic interactions. The energy harvester is built from an elastic beam connected to an electric circuit by a magnetostrictive material that promotes energy transduction. Besides, magnetic interactions define the system stability characterizing multistable configurations. The adaptiveness is provided by magnets that can change their position with respect to the beam, changing the system configuration. A mathematical model is proposed considering a novel model to describe magnetic interactions based on the single-point magnet dipole method, but employing multiple points to represent the magnetic dipole, which is more effective to match experimental data. The adaptive behavior allows one to alter the system stability and therefore, its dynamical response. A nonlinear dynamics analysis is performed showing the possibilities to enhance energy harvesting capacity from the magnet position change. The strategy is to perform a system dynamical characterization and afterward, alter the energetic barrier according to the environmental energy sources. Results show interesting conditions where energy harvesting capacity is dramatically increased by changing the system characteristics.

Keywords: adaptive systems; magnetic interaction; mechanical energy harvesting; nonlinear dynamics; smart materials

1. Introduction

The technology for power generation is a subject of essential importance in the 21st century due to either the everyday needs or the urgent search for renewable energies. In particular, these technologies have an increasing importance due to the growing use of mobile devices and the cell phone is an emblematic example with the increasing demand for phone signal, the use of internet, and mainly, batteries. The internet of things is another emblematic example that demands energy in remote places, but it also includes aerospace and oil & gas applications.

In this regard, there is an incessant search for solutions that can provide energy in a decentralized way. A solution that has been extensively studied is the energy harvesting, which is capable to collect available environmental energy, converting it for use (Erturk and Inman 2011a). Different kinds of energies are available in the environment, including solar, thermal and wind. Mechanical energy is an essential kind that can be exploited such as vibrations, deformations, pressures, and the human movement itself (Daqaq *et al*. 2020, Liu *et al*. 2021).

Energy harvesting is performed by some harvester device that converts the environmental energy into electrical energy. Smart materials are the essential component to perform the energy conversion. In essence, these materials have multiphysics couplings that confer adaptive behavior to engineering systems (Lopes Jr. *et al*. 2016). Typically, smart materials are able to convert mechanical into electrical energy, for instance, exploiting the electro-mechanical coupling. Piezoelectric and magnetostrictive materials are examples of smart materials usually employed for energy harvesting purposes (Rashidi *et al*. 2021, Narita and Fox 2018).

Energy harvesting systems are vast in the literature (Vallem *et al*. 2021, Liu *et al*. 2021, Narita and Fox 2018). A shoe equipped with a piezoelectric element in its insole can generate electrical energy from walking (Kymissis *et al*. 1998). Gym equipments that collect energy from human exercises are possible, as verified in some Fitness Club as Rochester (New York, NY) and Greenasium (San Diego, CA). Another interesting application is the use of smart materials in the floor to collect energy, which includes night clubs (Watt, Rotterdam; Surya, London) and roads. An important use of energy harvesting systems is to provide energy for sensors and actuators. In this regard, structural health monitoring is an essential kind of approach for wireless applications in engineering systems (Cahill *et al*. 2018, Kin and Na 2013, Casciati *et al*. 2012, Casciati and Rossi 2007).

One of the challenges for the design of energy harvesting systems is to deal with uncertainties and variabilities associated with environmental energy sources. The classical energy harvester is an elastic cantilever beam and its linear characteristic presents good performance under resonant conditions. Nevertheless, this performance can dramatically vary due to external variabilities.

*Corresponding author, Ph.D., Professor,
E-mail: savi@mecanica.coppe.ufrj.br

http://www.techno-press.org/?journal=sss&subpage=7
ISSN: 1738-1584 (Print), 1738-1991 (Online)

Therefore, adaptive behavior is needed to adjust system characteristics and make it feasible for the energy harvesting goals, seeking for good performance under different energy source conditions. The literature presents different configurations of vibration-based energy harvesting devices including broadband and multidirectional systems. In essence, different designs, shapes and multiple degrees of freedom are employed imagining the best performance configurations (Wang 2023; Zou *et al*. 2019, Erturk and Inman 2009, Kita *et al*. 2015). Fig. 1 presents some examples of novel ideas for energy harvesters: a pizza-shaped irregular structure that is a multi-degrees of freedom device that establishes a broadband response (Caetano and Savi 2021) (Fig. 1(a)); a star-shaped structure exploiting the same idea (Caetano and Savi 2022) (Fig. 1(b)); the incorporation of pendulum masses that aggregates multidirectionality to the device, providing a broadband and multi-direction response (Caetano and Savi 2022) (Fig. 1(b)); dual-beam design combining multiple degrees of freedom and compactness (Costa and Savi 2023, Costa *et al*. 2024, Krishnasamy *et al*. 2018, Wu *et al*. 2014) (Fig. 1(d)).

Nonlinearities and randomness are essential aspects to be exploited for the performance improvement of energy harvesters (Zou *et al*. 2019, Ghodsi *et al*. 2019, Cellular *et al*. 2018, Liu *et al*. 2021, Trentadue *et al*. 2019, De Paula *et al*. 2015). Nonsmooth nonlinearity is one possible strategy aiming to increase the device frequency range, exploiting impacts and other discontinuous behaviors (Ai *et al*. 2019). Advanced strategies can be imagined exploiting the synergistic use of smart materials that allows the combination of the best properties of each one of them, enhancing the energy harvesting capacity. In this regard, it should be pointed out the combination of piezoelectric materials with shape memory alloys as a promising alternative that uses the adaptive behavior to enhance energy harvesting capacity (Adeodato *et al*. 2021, Silva *et al*. 2015).

Nonlinear systems with distinct multistable aspects have been vastly employed exploiting either buckling or magnetic interactions (Osinaga *et al*. 2022, Lallart *et al*. 2019, Lan Qin, 2017). The literature presents different approaches to describe magnetic interactions, using either a Duffing-type polynomial (Zhou *et al*. 2013, De Paula *et al*. 2015) or other polynomial calibrated from experimental data (Cao *et al*. 2015a, b). Nevertheless, the most coherent approach treats magnetic interactions from the forces between magnets. Magnetic forces can be modeled by a single-point dipole approach (Aboulfotoh *et al*. 2013, Leng *et al*. 2017, Stanton *et al*. 2010), but Wang *et al*. (2020) proposed a two-point dipole showing that this new approach presents better representations of experimental data.

Multistable systems are interesting possibilities that create different equilibrium configurations that can be explored to increase energy harvesting capacity (Costa *et al*. 2021, 2024). Nevertheless, these systems are associated with energetic barriers that need to be overcome in order to reach interesting behaviors for energy harvesting (Cottone *et al*. 2012, Erturk and Inman 2011b). On this basis, the energy source needs to have an energy level high enough for a good harvesting performance since low energy levels impose situations where the system cannot overcome energetic barriers, presenting a poor performance (Daqaq *et al*. 2014). The performance improvement of multistable energy harvesting systems is related to the capacity to overcome the energetic barriers (Norenberg *et al*. 2023, Yang and Towfighian 2017, Lan and Qin 2017). Therefore, nonlinear dynamics perspective is essential for the proper design of multistable energy harvesting systems (Costa *et al*. 2021, 2024, Costa and Savi 2023). In addition, the use of

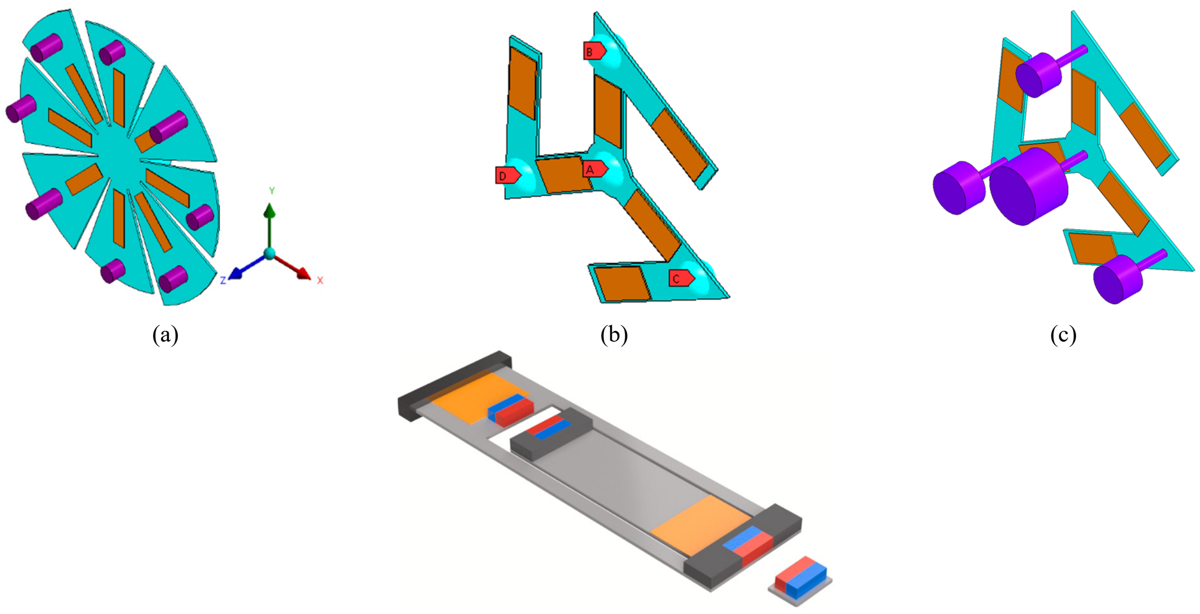

(d)

Fig. 1 Different configurations of energy harvesting devices: (a) pizza-shaped device (Caetano and Savi 2021); (b) star-shaped device (Caetano and Savi 2022); (c) star-shaped device with pendulum masses (Caetano and Savi 2022); (e) compact dual-beam (Costa and Savi 2023, Costa *et al*. 2024) control strategies can be useful to design adaptive systems and chaos control is of special interest due to its low energy consumption (Barbosa *et al*. 2015).

This work investigates mechanical energy harvesting systems using smart materials and adaptiveness. The main motivation is to propose a smart, adaptive, multistable energy harvesting system capable of changing energetic barriers, allowing better performance for different environmental energy sources. Magnetostrictive transduction is employed to promote electro-mechanical conversion, establishing an interesting alternative to the usual piezoelectric transduction. Multistability is provided by magnetic interactions that can be altered through the movement of magnets, conferring adaptive characteristics due to changes in the energetic barrier. A mathematical model is developed considering a novel magnetic interaction model based on the single-point dipole methodology, but using multiple points to represent the magnetic interactions, which combines effectiveness and simplicity. On this basis, it is proposed a novel energy harvesting device composed by a multistable elastic beam with magnetostrictive transduction and adaptive behavior provided by magnet interactions. The configuration changes are guided by dynamical perspective, allowing one to predict the most suitable operational conditions according to the environmental sources. Numerical simulations are carried out showing some interesting situations where adaptability allows a better performance.

2. Energy harvesting system

The proposed energy harvesting device is a smart and adaptive system composed by an elastic beam, with a magnet tip mass, interacting with a system of three magnets that can change its position, and subjected to a base excitation that represents the environmental energy source, Fig. 2. Based on the first vibration mode, it is possible to treat this system as a one degree of freedom electro-mechanical oscillator also presented in Fig. 2.

Energy transduction is provided by a megnetostrictive material, a smart material with magneto-mechanical coupling. Therefore, the elastic beam is connected to an electric circuit by a megnetostrictive material associated with a coil that promotes the electro-magnetic conversion. Although piezoelectric transduction is the most common mechanism employed in the literature, magnetostrictive material is an interesting alternative that can present a more effective energy density transduction depending on the system characteristics. Similar construction and modeling aspects are identified for typical energy harvesters with these two transduction mechanisms.

On this basis, the dimensionless equations of motion are written assuming that z is the relative displacement and i is the electric current (Erturk and Inman 2011a, Engdahl and Quandt 2000)

$$\begin{aligned} &\ddot{z} + 2\xi\omega_n\,\dot{z} + \omega_n^2\,z - \Theta i = f_{ext} + f_{mag} \\ &\frac{1}{L}(R\,i - \Theta\,\dot{z}) = 0 \end{aligned} \qquad (1)$$

where ξ is the dissipation coefficient, $\omega_n = \sqrt{k/M}$ is the natural frequency associated with the linear system; k is the stiffness and M is the mass; Θ is the magneto-mechanical coupling coefficient, R is the electrical resistance, L is the inductance. Magnetic interactions are modeled by considering four magnets: one is the tip mass O, and the others are represented by L (left), C (center) and R (right). Moreover, the position of the central magnet C can alter its position, defined by x_{im}. The horizontal distance of the magnets C-L and C-R is d_g (z-direction). Besides, the distance between the tip mass O and the center magnet C is given by $d = d_0 + x_{im}$; $f_{mag} = F_{mag}/M$ is related to the magnetic force, described in the sequel; $f_{ext} = A_0\cos(\omega t)$ is the external stimulus that represent the energy source.

The energy harvesting capacity is monitored by the average power estimated by the root mean square (rms)

$$P_{rms} = \sqrt{\frac{1}{(t_2 - t_1)}\int_{t_1}^{t_2} P^2\,dt} \qquad (2)$$

where $P = P(t) = R\,i^2$.

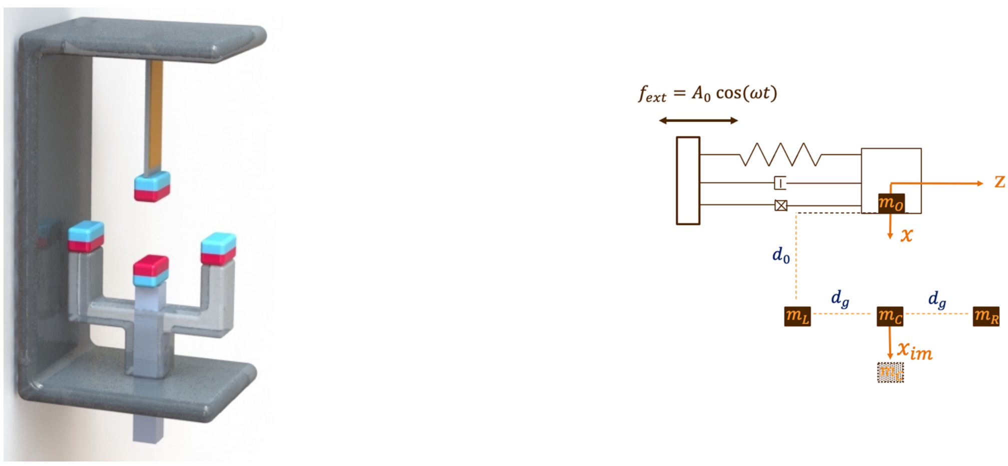

Fig. 2 Smart, adaptive energy harvesting system showing the three-dimensional representation and the equivalent nonlinear oscillator

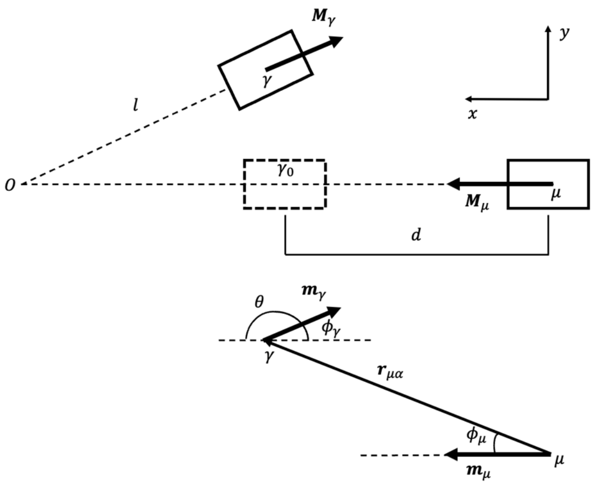

Fig. 3 Magnetic interactions modeled from the equivalent point dipole method (Tan *et al.* 2017)

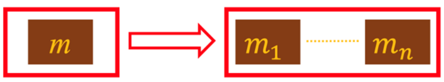

Fig. 4 Multipoint representation of each magnet

2.1 Magnetic interactions

There are different alternatives to model magnetic interactions. A polynomial fit is an alternative that is usually represented by the Duffing-type cubic equation (Zhou *et al.* 2013), but there are other alternatives related to different polynomials (Cao *et al.* 2015a, b). A more consistent approach uses the magnetic field interactions. Aboulfotoh *et al.* (2013), Leng *et al.* (2017), Stanton *et al.* (2010) and Tan *et al.* (2015) exploited the equivalent single-point dipole method (Fig. 3). Wang *et al.* (2019, 2020) proposed a more sophisticated approach representing the magnet by two points, which presents better fits with experimental data.

A novel model is here proposed by considering the single-point dipole method but using multiple points to represent the dipole. On this basis, each dipole is represented by a sequence of points allowing a better representation that presents a smoother force field. Therefore, each magnet is represented by n points as illustrated in Fig. 4.

In this regard, consider the magnetic interaction between two magnets (Fig. 2), γ and μ, assuming that bold letters denote vector/tensor quantities

$$\boldsymbol{B}_{\gamma\mu} = -\frac{\mu_0}{4\pi}\nabla\frac{\boldsymbol{m}_\mu\cdot\boldsymbol{r}_{\gamma\mu}}{r_{\gamma\mu}^3} \tag{3}$$

where ∇ is the nabla operator, μ_0 is the permissibility, $\boldsymbol{m}_\mu$ is the dipole magnetic moment that is associated with the magnet μ. Vector $\boldsymbol{r}_{\gamma\mu}$ is the source of the magnetic moment from μ to γ. The potential energy is given by

$$U_m = -\boldsymbol{B}_{\gamma\mu}\cdot\boldsymbol{m}_\mu = -\frac{\mu_0}{4\pi}\nabla\frac{\boldsymbol{m}_\gamma\cdot\boldsymbol{r}_{\gamma\mu}}{r_{\gamma\mu}^3}\cdot\boldsymbol{m}_\mu \tag{4}$$

The magnetic force on the dipole μ imposed by dipole γ is the following

$$\boldsymbol{F} = -\nabla U_m = -\frac{\mu_0}{4\pi}\nabla\left[\left(\nabla\frac{\boldsymbol{m}_\gamma\cdot\boldsymbol{r}_{\gamma\mu}}{r_{\gamma\mu}^3}\right)\cdot\boldsymbol{m}_\mu\right] \tag{5}$$

Tan *et al.* (2015) showed that this equation can be simplified as follows

$$\begin{aligned}\boldsymbol{F} = \frac{3\mu_0 m_\mu m_\gamma}{4\pi r_{\gamma\mu}^4}\big[&\hat{\boldsymbol{r}}_{\gamma\mu}(\hat{\boldsymbol{m}}_\mu\cdot\hat{\boldsymbol{m}}_\gamma)+\hat{\boldsymbol{m}}_\gamma(\hat{\boldsymbol{m}}_\mu\cdot\hat{\boldsymbol{r}}_{\gamma\mu})\\ &+\hat{\boldsymbol{m}}_\mu(\hat{\boldsymbol{m}}_\gamma\cdot\hat{\boldsymbol{r}}_{\gamma\mu})\\ &-5\hat{\boldsymbol{r}}_{\gamma\mu}(\hat{\boldsymbol{m}}_\mu\cdot\hat{\boldsymbol{r}}_{\gamma\mu})(\hat{\boldsymbol{m}}_\gamma\cdot\hat{\boldsymbol{r}}_{\gamma\mu})\big]\end{aligned} \tag{6}$$

where $\hat{\boldsymbol{m}}_\mu, \hat{\boldsymbol{m}}_\gamma, \hat{\boldsymbol{r}}_{\gamma\mu}$ represent the unit vectors on the direction of $\boldsymbol{m}_\alpha, \boldsymbol{m}_\gamma, \boldsymbol{r}_{\gamma\mu}$, respectively. In general, the force can be expressed by $\boldsymbol{F} = F_x\,\boldsymbol{i} + F_z\,\boldsymbol{k}$ and x-direction term can be neglected (Tan *et al.* 2015). By performing a discretization of each dipole using n points, it is possible to express each force by the equation

$$F_{\gamma\mu\,z} = \frac{1}{n}\sum_{\alpha=1}^{n}F_{\gamma\mu\,\alpha} \tag{7}$$

The potential energy of the energy harvesting device, U, is defined by combining the beam potential energy, $U_p = \frac{1}{2}kz^2$, and the magnet interactions, $U_m = \int_{z_1}^{z_2}F_z\,dz$: $U = U_p + U_m$. Therefore, based on the same multipoint approach, the magnetic energy can be expressed by

$$U_m = \frac{1}{n}\sum_{\alpha=1}^{n}U_{\gamma\mu\,\alpha} \tag{8}$$

Under these assumptions and considering $n = 3$, each magnetic force is written as follows

$$\begin{aligned}F_{\beta O\alpha} &= \frac{3\mu_0 m_O m_\beta}{4\pi r_{\beta O}^4}\Bigg[-\frac{(z+\varsigma_\beta d_g+\psi_\alpha d_i)}{r_{jO}}\cos\theta+\frac{d_0}{r_{\beta O}}\sin\theta\\ &\qquad -5\,d_0\frac{(z+\varsigma_\beta d_g+\psi_\alpha d_i)}{r_{\beta O}^2}\left(-\frac{d_0}{r_{\beta O}}\cos\theta+\frac{z+\varsigma_\beta\,d_g+\psi_\alpha d_i}{r_{\beta O}}\sin\theta\right)\Bigg]\\ F_{CO\alpha} &= \frac{3\mu_0 m_O m_C}{4\pi r_{CO}^4}\left[-\frac{(z+\psi_\alpha d_i)}{r_{CO}}\cos\theta+\frac{d}{r_{CO}}\sin\theta-5d\,\frac{(z+\psi_\alpha d_i)}{r_{CO}^2}\left(-\frac{d}{r_{CO}}\cos\theta+\frac{z+\psi_\alpha d_i}{r_{CO}}\sin\theta\right)\right]\end{aligned} \tag{9}$$

where the following definitions were adopted

$$\varsigma_\beta = \begin{cases} -1 & \text{if} \quad \beta = L \\ +1 & \text{if} \quad \beta = R \end{cases}$$
$$\psi_\alpha^{(n=3)} = \begin{cases} -1 & \text{if} \ \alpha = 1 \\ 0 & \text{if} \ \alpha = 2 \\ +1 & \text{if} \ \alpha = 3 \end{cases} \tag{10}$$

Note that the definition of ψ_α depends on the number of points employed to represent the dipole, n. These expressions consider the definition of the following parameters

$$r_{LO} = \sqrt{\left(z - d_g\right)^2 + d_0^2}$$
$$r_{RO} = \sqrt{\left(z + d_g\right)^2 + d_0^2}$$
$$r_{CO} = \sqrt{z^2 + d^2} \tag{11}$$
$$\cos\theta = \frac{\sqrt{l^2 - z^2}}{l}$$
$$\sin\theta = \frac{z}{l}$$

Based on that, the force on magnet O, the tip mass, is given by

$$F_{mag} = F_{LOz} + F_{COz} + F_{ROz} \tag{12}$$

Therefore, remembering that it is assumed $n = 3$, each of the forces is written by

$$F_{mag} = \frac{1}{3}\left(F_{LO1} + F_{LO2} + F_{LO3}\right) + \frac{1}{3}\left(F_{RO1} + F_{RO2} + F_{RO3}\right) + \frac{1}{3}\left(F_{CO1} + F_{CO2} + F_{CO3}\right) \tag{13}$$

In addition, the energy is given by, $U_m = \frac{1}{3}\left(U_{LO1} + U_{LO2} + U_{LO3} + U_{RO1} + U_{RO2} + U_{RO3} + U_{CO1} + U_{CO2} + U_{CO3}\right)$, associated with the following expressions

Table 1 Energy harvesting system parameters (Tan *et al.* 2017)

d_0 [mm]	2.5
d_g [mm]	6.3
d_i [mm]	0.8
x_{im} [mm]	[-0.3, 0.0, 0.3, 1.5]
ω_n [rad/s]	161.91
Θ [N/V]	0.1203
ξ	0.02
A_0 [m/s^2]	10
ω [rad/s]	161.91
m_O [A m^2]	0.015
$m_{L,R}$ [A m^2]	0.015
m_C [A m^2]	0.006
l	102.85

associated with distinct kinds of responses that are used to define the patterns for adaptive behavior. Costa *et al.* (2021) showed that nonlinear dynamics perspective is an essential point that should be employed to evaluate the energy harvesting device design.

Dynamical characterization is carried out by establishing a dynamical map of the energy harvester. Each kind of behavior is characterized by a dynamical pattern represented by the energy curve, which establishes the stability condition (mono, bi or tristable); phase space together with Poincaré map, and displacement time history, which show the dynamical response and its pattern. Each dynamical pattern is associated with an energy harvesting capacity expressed by the harvested RMS power calculated for steady state behavior, discharging the transient period.

Fig. 5 presents results generated with an initial condition $z_0 = -8$ mm and distinct positions of the magnets,

$$U_{\beta O\alpha} = \frac{\mu_0 m_O m_\beta}{4\pi r_{\beta O}^3}\left[\frac{3d_0^2}{r_{\beta O}^2}\cos\theta - \frac{3\left(z + \varsigma_\beta d_g + \psi_\alpha d_i\right)d_0}{r_{\beta O}^2}\sin\theta - \cos\theta\right]$$
$$U_{CO\alpha} = \frac{\mu_0 m_O m_C}{4\pi r_{CO}^3}\left[\frac{3d^2}{r_{CO}^2}\cos\theta - \frac{3\left(z + \psi_\alpha d_i\right)d}{r_{CO}^2}\sin\theta - \cos\theta\right] \tag{14}$$

3. Numerical simulations

This section presents numerical simulations that are carried out employing the fourth-order Runge-Kutta method considering time steps less than $2\pi/300\omega$, defined after a convergence analysis. Parameters presented in Table 1 are employed for all simulations representing typical values for an elastic beam, magnetostrictive coupling, and magnetic interactions.

The analysis of the energy harvesting device starts with a dynamical characterization for different magnetic interactions promoted by distinct positions of the magnet C, defined by the distance x_{im}, which alters the distance *d*. The idea is to exploit different configurations that are represented by a panel with three subfigures. Initially, Fig. 5(a) presents an intra-well period-1 response ($d = 2.2$ mm; $x_{im} = -0.3$ mm), showing that the system is not able to overcome the energetic barrier and therefore, the state space is restricted to a position related to a specific potential well, which is also clear by observing the displacement time history. Due to that, the average collected power is small: $P_{rms} = 0.116\,\mu W$. Afterward, by considering $d = 2.5$ mm or $x_{im} = 0$, Fig. 5(b) presents a chaotic response visiting all wells. This kind of behavior has a dramatic increase on displacement values, which is associated with a bigger harvested power, $P_{rms} = 3.177\,\mu W$. By considering $d = 2.8$ mm or $x_{im} = 0.3$ mm, the system presents a high energy level, related to

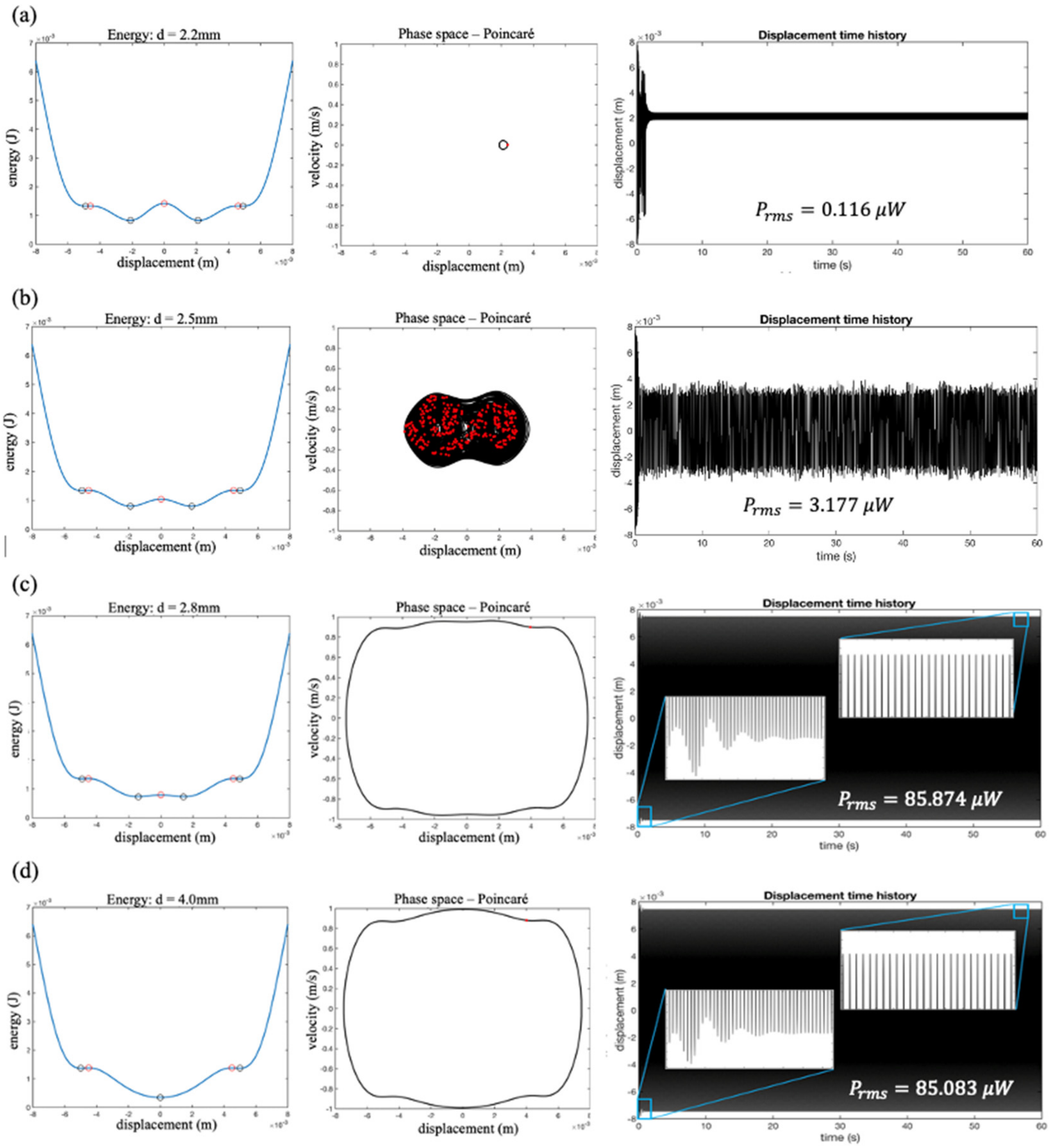

Fig. 5 Dynamical characterization of the energy harvester for different magnetic interactions defined by distance d promoted by changing the position of the C magnet, x_{im}: (a) $d = 2.2$ or $x_{im} = -0.3$ mm; (b) $d = 2.5$ or $x_{im} = 0$; (c) $d = 2.8$ or $x_{im} = 0.3$ mm; (d) $d = 4.0$ or $x_{im} = 1.5$ mm

an inter-well period-1 behavior (Fig. 5(c)). Note that the oscillatory time history response is represented by a black picture, and the depicted enlargements show details of the response that is associated with an average harvested power of $P_{rms} = 85.874\ \mu W$. The same qualitative behavior is achieved when $d = 4.0$ mm or $x_{im} = 1.5$ mm, presented in Fig. 5(d), which is associated with an average harvested power of $P_{rms} = 85.083\ \mu W$. This configuration is associated with a condition where the magnet C does not have influence on system dynamics.

It should be pointed out that the collected energy is dramatically increased from the first to the third cases, and the fourth case is compatible with the third one. This kind of changes motivate the idea of an adaptive device, where nonlinear dynamics guides the system changes. These changes can be understood as the seek for the best configurations to overcome the multistable energetic barriers provided by magnetic interactions.

On this basis, the major motivation of the adaptive system is to change system configuration based on dynamical patterns, named (*a*), (*b*), (*c*) and (*d*), according to Fig. 5. As a proof of concept, system configurations are now altered among the four discussed patterns, assuming that changes are performed instantaneously from one condition to the other. This can be understood as an ideal controller that alters the magnet position, changing the energy harvesting capacity. Different scenarios are considered by assuming an initial condition, $z_0 = -8$ mm. The first case starts with $x_{im} = 0.3$, a low energy situation associated with case (*a*). Fig. 6 shows the configuration changes at each 15s by considering two different sequences chosen based on the dynamical patterns discussed in Fig. 5. Initially, the sequence of dynamical patterns (*a*)-(*b*)-(*c*)-(*d*) is assumed and the system collects a power of $2.176\ \mu W$. On the other hand, a different sequence (*d*)-(*c*)-(*b*)-(*a*) dramatically increases the collected power to $86.162\ \mu W$.

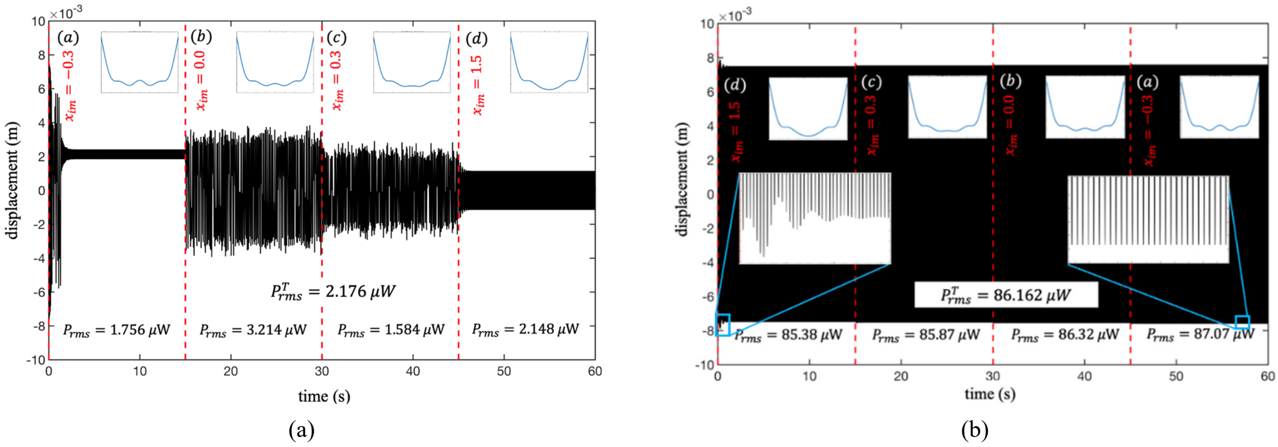

Fig. 6 Energy harvesting capacity considering different dynamical pattern sequences of adaptive behavior using $z_0 = -8$ mm. (a) Sequence (*a*)-(*b*)-(*c*)-(*d*); (b) Sequence (*d*)-(*c*)-(*b*)-(*a*)

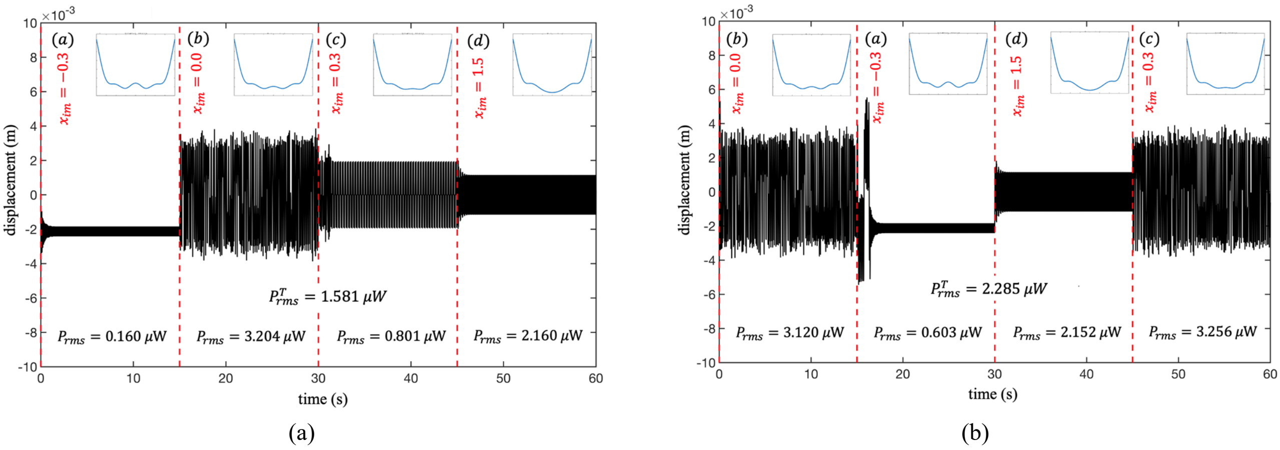

Fig. 7 Energy harvesting capacity considering different dynamical pattern sequences of adaptive behavior using $z_0 = -5$ mm. (a) Sequence (*a*)-(*b*)-(*c*)-(*d*); (b) Sequence (*b*)-(*a*)-(*d*)-(*c*)

These kinds of behaviors show the possibilities of the adaptive system for energy harvesting purposes.

A different initial condition is now of concern, allowing one to observe system sensitivity. By assuming $z_0 = -5$ mm, different sequences are analyzed and presented in Fig. 6. Initially, the sequence of dynamical patterns (*a*)-(*b*)-(*c*)-(*d*) is assumed and the system collects a power of $1.581\ \mu W$, significantly less than the previous case. By considering a different sequence (*b*)-(*a*)-(*d*)-(*c*), the collected power is increased to $2.285\ \mu W$. Once again, it is clear that the magnetic interaction variations are able to significantly enhance the energy harvesting capacity.

3.1 External stimulus frequency fluctuations

Energy source fluctuations are unavoidable, which make the design of energy harvesting devices a challenging topic. In order to show the use of the adaptive system under stimulus uncertainties, frequency fluctuations are of concern to represent the environmental energy source variations. Simulations with $z_0 = -5$ mm are considered as the reference case. Frequency variations assumes the following sequence established with respect to a natural frequency reference (Fig. 8): $0.75\omega_n, 0.85\omega_n, \omega_n, 1.25\omega_n$.

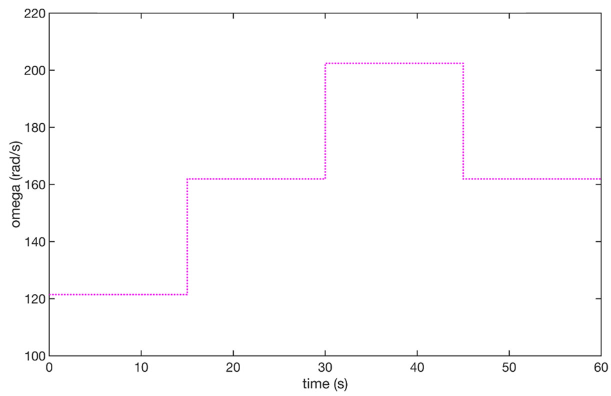

Fig. 8 Frequency fluctuations of the external stimulus that represents the energy source: $0.75\omega_n$, $0.85\omega_n$, ω_n, $1.25\omega_n$

By assuming that the device is not adaptive, the best configuration in terms of collected energy is represented by pattern (*c*). Fig. 9 presents simulations of the energy harvester for configuration associated with dynamical

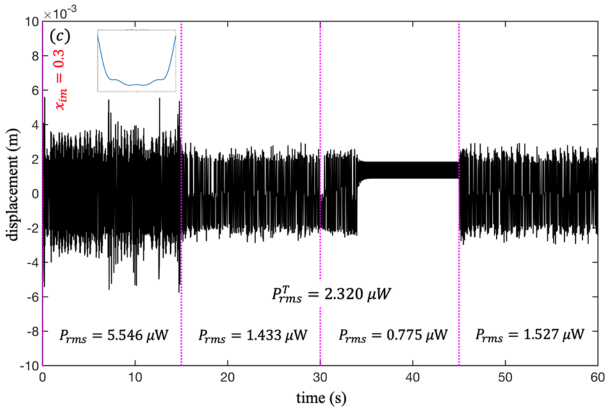

Fig. 9 Energy harvesting device response when subjected to frequency fluctuations working in configuration associated with pattern (c), $x_{im} = 0.3$

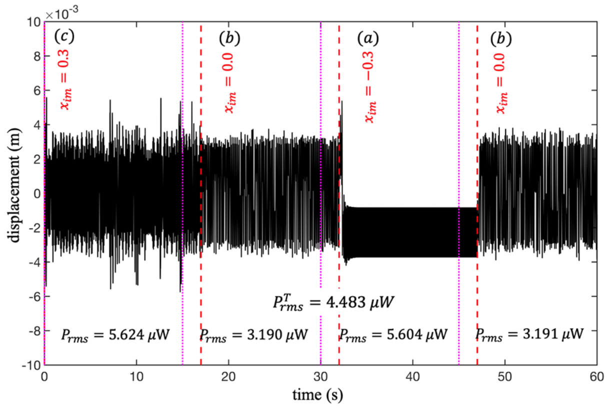

(a)

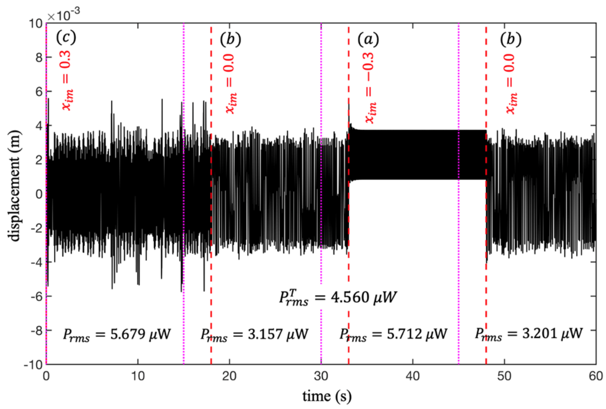

(b)

Fig. 10 Adaptive behavior employed to deal the frequency fluctuations of the external stimulus considering the dynamical pattern sequence (c)-(b)-(a)-(b) and two different time delays: (a) $\tau = 2\ s$; (b) $\tau = 3\ s$

pattern (c) ($x_{im} = 0.3$) and subjected to the frequency fluctuations showed in Fig. 8. Under these conditions, the system presents different displacement levels for each frequency, harvesting a total power of $2.320\ \mu W$. Note that the performance changes due to frequency variations suggesting that changes are interesting to enhance the energy harvesting capacity.

Adaptive behavior is now incorporated by considering configuration changes defined after a delay for the recognition of the frequency variation, represented by the delay time τ. In this regard, an ideal controller is of concern, instantaneously changing the configuration after a delay time. The configuration change follows the sequence of dynamical patterns: (c)-(b)-(a)-(b). Results of these configuration changes are presented in Fig. 10. By assuming a delay time $\tau = 2$s (Fig. 10(a)), the device collects $4.483\ \mu W$, showing a significantly enhancement of the energy harvesting capacity with respect to the previous case. On the other hand, by considering a delay time $\tau = 3$ s (Fig. 10(b)), the system collects $4.560\ \mu W$, even better than the case $\tau = 2$ s. The difference of results related to distinct delay times is due to the strong sensitivity to initial conditions. Since configuration changes are related to different time instants, the displacement is different for each case, being enough to alter the system response. This shows that a deep understanding of the nonlinear dynamics is an essential point for a proper design and definition of the best strategy for configuration changes. In this regard, it is important to further develop a proper strategy for the design of a nonlinear controller to define the adaptive sequence.

4. Conclusions

This paper proposes a smart, adaptive, multistable energy harvesting system with magnetic interactions. The energy transduction is provided by magnetostrictive materials. The adaptive behavior is provided by the movement of magnets that alters energetic barriers and changes the energy harvesting capacity. A mathematical model is proposed using a novel model to describe magnetic interactions based on equivalent single-point dipole method but considering several points to have a smoother description. This approach combines the effectiveness to describe magnetic interactions with simplicity. Nonlinear dynamics of the energy harvester is carried out establishing the characteristics of the system, defining dynamical patterns employed to guide adaptive behavior. Results show that energetic barriers can be properly overcome by considering appropriate configuration changes based on the dynamical patterns. Numerical simulations present a proof of concept showing the enhancement of energy harvesting capacity by altering the system configurations. Besides, this strategy is evaluated considering frequency fluctuations of the environmental energy sources, showing that proper changes can deal with uncertainties. The main conclusion is that nonlinear dynamics is the essential point to guide adaptive actuations, promoting better performance of the energy harvesters.

Acknowledgments

The authors would like to acknowledge the support of the Brazilian Research Agencies CNPq (Conselho Nacional de Desenvolvimento Científico e Tecnológico), CAPES

(Coordenação de Aperfeiçoamento de Pessoal de Nível Superior) and FAPERJ (Fundação Carlos Chagas Filho de Amparo à Pesquisa do Estado do Rio de Janeiro) and through the INCT-EIE (National Institute of Science and Technology - Smart Structures in Engineering), CNPq, CAPES and FAPEMIG (Fundação de Amparo à Pesquisa do Estado de Minas Gerais). The support of the AFOSR (Air Force Office of Scientific Research) is also acknowledged.

References

Aboulfotoh, N.A., Arafa, M.H. and Megahed, S.M. (2013), "A self-tuning resonator for vibration energy harvesting", *Sensors Actuat. A*: *Phys*., **201**, 328-334. https://doi.org/10.1016/j.sna.2013.07.030

Adeodato, A., Duarte, B.T., Monteiro, L.L.S., Pacheco, P.M. and Savi, M.A. (2021), "Synergistic use of piezoelectric and shape memory alloy elements for vibration-based energy harvesting", *Int*. *J*. *Mech*. *Sci*., **194**, p. 106206. https://doi.org/10.1016/j.ijmecsci.2020.106206

Ai, R., Silva Monteiro, L.L., Monteiro Jr., P.C.C., Pacheco, P.M. and Savi, M.A. (2019), "Piezoelectric vibration-based energy harvesting enhancement exploiting nonsmoothness", *Actuators*, **8**(1), p. 25. https://doi.org/10.3390/act8010025

Barbosa, W.O.V., De Paula, A.S., Savi, M.A. and Inman, D.J. (2015), "Chaos control applied to piezoelectric vibration-based energy harvesting systems", *Eur*. *Phys*. *J*. – *Special Topics*, **224**(14-15), 2787-2801. https://doi.org/10.1140/epjst/e2015-02589-1

Caetano, V.J. and Savi, M.A. (2021), "Multimodal pizza-shaped piezoelectric vibration-based energy harvesters", *J*. *Intell*. *Mater*. *Syst*. *Struct*., **32**(20), 2505-2528. https://doi.org/10.1177/1045389X211006910

Caetano, V.J. and Savi, M.A. (2022), "Star-shaped piezoelectric mechanical energy harvesters for multidirectional sources", *Int*. *J*. *Mech*. *Sci*., **215**, p. 106962. https://doi.org/10.1016/j.ijmecsci.2021.106962

Cahill, P., Pakrashi, V., Sun, P., Mathewson, A. and Nagarajaiah, S. (2018), "Energy harvesting techniques for health monitoring and indicators for control of a damaged pipe structure", *Smart Struct*. *Syst*., *Int*. *J*., **21**(3), 287-303. https://doi.org/10.12989/sss.2018.21.3.287

Cao, J., Zhou, S., Inman, D.J. and Chen, Y. (2015a), "Chaos in the fractionally damped broadband piezoelectric energy generator", *Nonlinear Dyn*., **80**(4), 1705-1719. https://doi.org/10.1007/s11071-014-1320-6

Cao, J., Zhou, S., Wang, W. and Lin, J. (2015b), "Influence of potential well depth on nonlinear tristable energy harvesting", *Appl*. *Phys*. *Lett*., **106**, p. 173903. https://doi.org/10.1063/1.4919532

Casciati, F. and Rossi, R. (2007), "A power harvester for wireless sensing applications", *Struct*. *Control Health Monitor*., **14**, 649-659. https://doi.org/10.1002/stc.179

Casciati, S., Faravelli, L. and Chen, Z. (2012), "Energy harvesting and power management of wireless sensors for structural control applications in civil structures", *Smart Struct*. *Syst*., *Int*. *J*., **10**(3), 299-312. https://doi.org/10.12989/sss.2012.10.3.299

Cellular, A.C.S., Monteiro, L.L.S. and Savi, M.A. (2018), "Numerical investigation of nonlinear mechanical and constitutive effects on piezoelectric vibration-based energy harvesting", *Technisches Messen* / *Technical Measurements*, **85**(9), 565-579. https://doi.org/10.1515/teme-2017-0070

Chen, B., Li, S., Tang, X. and Zhang, L. (2021), "A study of a new hybrid vibration energy harvester based on broadband-multimode", *Smart Struct*. *Syst*., *Int*. *J*., **28**(1), 29-41. https://doi.org/10.12989/sss.2021.28.1.029

Costa, L.G. and Savi, M.A. (2023), "Nonlinear dynamics of a compact and multistable mechanical energy harvester", *Int*. *J*. *Mech*. *Sci*., **262**, p. 108731. https://doi.org/10.1016/j.ijmecsci.2023.108731

Costa, L.G., Monteiro, L.L.S., Pacheco, P.M. and Savi, M.A. (2021), "A parametric analysis of the nonlinear dynamics of bistable vibration-based piezoelectric energy harvesters", *J*. *Intell*. *Mater*. *Syst*. *Struct*., **32**(7), 699-723. https://doi.org/10.1177/1045389X20963188

Costa, L.G., Monteiro, L.L.S. and Savi, M.A. (2024), "Multistability investigation for improved performance in a compact nonlinear energy harvester", *J*. *Brazil*. *Soc*. *Mech*. *Sci*. *Eng*., **46**, p. 212. https://doi.org/10.1007/s40430-024-04766-5

Cottone, F., Gammaitoni, L., Vocca, H. and Ferrari, V. (2012), "Piezoelectric buckled beams for random vibration energy harvesting", *Smart Mater*. *Struct*., **21**(3), 1-11. https://doi.org/10.1088/0964-1726/21/3/035021

Daqaq, M.F., Masana, R., Erturk, A. and Quinn, D.D. (2014), "On the role of nonlinearities in vibratory energy harvesting: a critical review and discussion", *Appl*. *Mech*. *Rev*., **66**, p. 040801. https://doi.org/10.1115/1.4026278

Daqaq, M.F., Crespo, R.S. and Ha, S. (2020), "On the efficacy of charging a battery using a chaotic energy harvester", *Nonlinear Dyn*., **99**, p. 1525. https://doi.org/10.1007/s11071-019-05372-0

De Paula, A.S., Inman, D.J. and Savi, M.A. (2015), "Energy harvesting in a nonlinear piezomagnetoelastic beam subjected to random excitation", *Mech*. *Syst*. *Signal Process*., **54**, 405-416. https://doi.org/10.1016/j.ymssp.2014.08.020

Engdahl, G. and Quandt, E. (2000), "Handbook of Giant Magnetostrictive Materials", San Diego Press, Academic.

Erturk, A. and Inman, D.J. (2009), "An experimentally validated bimorph cantilever model for piezoelectric energy harvesting from base excitations", *Smart Mater*. *Struct*., **18**, p. 025009. https://doi.org/10.1088/0964-1726/18/2/025009

Erturk, A. and Inman, D.J. (2011a), *Piezoeletric Energy Harvesting*, John Wiley & Sons.

Erturk, A. and Inman, D.J. (2011b), "Broadband piezoelectric power generation on high-energy orbits of the bistable Duffing oscillator with electromechanical coupling", *J*. *Sound Vib*., **330**, 2339-2353. https://doi.org/10.1016/j.jsv.2010.11.018

Ghodsi, M., Ziaiefar, H., Mohammadzaheri, M., Omar, F.K. and Bahadur, I. (2019), "Dynamic analysis and performance optimization of permendur cantilevered energy harvester", *Smart Struct*. *Syst*., *Int*. *J*., **23**(5), 421-428. https://doi.org/10.12989/sss.2019.23.5.421

Kim, S. and Na, U. (2013), "Energy harvesting techniques for remote corrosion monitoring systems", *Smart Struct*. *Syst*., *Int*. *J*., **11**(5), 555-567. https://doi.org/10.12989/sss.2013.11.5.555

Kita, S., Ueno, T. and Yamada, S. (2015), "Improvement of force factor of magnetostrictive vibration power generator for high efficiency", *J*. *Appl*. *Phys*., **117**, p. 17B508. https://doi.org/10.1063/1.4907237

Krishnasamy, M., Upadrashta, D., Yang, Y. and Lenka, T.R. (2018), "Distributed parameter modelling of cutout 2-DOF cantilevered piezo-magneto-elastic energy harvester", *J*. *Microelectromech*. *Syst*., **27**(6), 1160-1170. https://doi.org/10.1109/JMEMS.2018.2875788

Kymissis, J., Kendall, C., Paradiso, J. and Gershenfeld, N. (1998), "Parasitic Power Harvesting in Shoes", In: *IEEE International Conference on Wearable Computing*, ver. 2. https://doi.org/10.1109/ISWC.1998.729539

Lallart, M., Zhou, S., Yan, L., Yang, Z. and Chen, Y. (2019), "Tailoring multistable vibrational energy harvesters for enhanced performance: theory and numerical investigation", *Nonlinear Dyn*., **96**, p. 1283.

https://doi.org/10.1007/s11071-019-04853-6
Lan, C. and Qin, W. (2017), “Enhancing ability of harvesting energy from random vibration by decreasing the potential barrier of bistable harvester”, *Mech. Syst. Signal Process.*, **85**, 71-81. https://doi.org/10.1016/j.ymssp.2016.07.047
Leng, Y., Tan, D., Liu, J., Zhang, Y. and Fan, S. (2017), “Magnetic force analysis and performance of a tri-stable piezoelectric energy harvester under random excitation”, *J. Sound Vib.*, **406**, 146-160. https://doi.org/10.1016/j.jsv.2017.06.020
Liu, L., Guo, X., Liu, W. and Lee, C. (2021), “Recent progress in the energy harvesting technology-from self-powered sensors to self-sustained IoT, and new applications”, *Nanomaterials*, **11**(11), p. 2975. https://doi.org/10.3390/nano11112975
Lopes Jr, V., Steffen Jr, V. and Savi, M.A. (2016), *Dynamics of Smart Systems and Structures*, Springer.
Narita, F. and Fox, M. (2018), “A review on piezoelectric, magnetostrictive, and magnetoelectric materials and device technologies for energy harvesting applications”, *Adv. Eng. Mater.*, **20**(5), p. 1700743. https://doi.org/10.1002/adem.201700743
Norenberg, J.P., Luo, R., Lopes, V.G., Peterson, J.V.L. and Cunha, A. (2023), “Nonlinear dynamics of asymmetric bistable energy harvesters”, *Int. J. Mech. Sci.*, **257**, p. 108542. https://doi.org/10.1016/j.ijmecsci.2023.108542
Osinaga, S., Machado, S. and Febbo, M. (2022), “An analytical model of the electromechanical coupling for a piezoelectric stepped buckled beam for energy harvesting applications”, *Mech. Syst. Signal Process.*, **179**, p. 109355. https://doi.org/10.1016/j.ymssp.2022.109355
Rashidi, S., Ehsani, M.H., Shakouri, M. and Karimi, N. (2021), “Potentials of magnetic shape memory alloys for energy harvesting”, *J. Magnet. Magnet. Mater.*, **537**, p. 168112. https://doi.org/10.1016/j.jmmm.2021.168112
Silva, L.L., Oliveira, S.A., Pacheco, P.M. and Savi, M.A. (2015), “Synergistic use of smart materials for vibration-based energy harvesting”, *Eur. Phys. J. – Special Topics*, **224**(14-15), 3005-3012. https://doi.org/10.1140/epjst/e2015-02603-8
Stanton, S.C., Mcgehee, C.C. and Mann, B.P. (2010), “Nonlinear dynamics for broadband energy harvesting: Investigation of a bistable piezoelectric inertial generator”, *Physica D: Nonlinear Phenomena*, **239**, 640-653. https://doi.org/10.1016/j.physd.2010.01.019
Tan, D., Leng, Y.G. and Gao, Y.J. (2015), “Magnetic force of piezoelectric cantilever energy harvesters with external magnetic field”, *Eur. Phys. J. - Special Topics*, **224**, 2839-2853. https://doi.org/10.1140/epjst/e2015-02592-6
Trentadue, F., Quaranta, G., Maruccio, C. and Marano, G.C. (2019), “Energy harvesting from piezoelectric strips attached to systems under random vibrations”, *Smart Struct. Syst., Int. J.*, **24**(3), 333-343. https://doi.org/10.12989/sss.2019.24.3.333
Vallem, V., Sargolzaeiaval, Y., Ozturk, M., Lai, Y.-C. and Dickey, M.D. (2021), “Energy harvesting and storage with soft and stretchable materials”, *Adv. Mater.*, **33**, p. 2004832. https://doi.org/10.1002/adma.202004832
Wang, T. (2023), “Pendulum-based vibration energy harvesting: Mechanisms, transducer integration, and applications”, *Energy Convers. Manag.*, **276**, p. 116469. https://doi.org/10.1016/j.enconman.2022.116469
Wang, G., Liao, W-H., Zhao, Z., Tan, J., Cui, S., Wu, H. and Wang, W. (2019), “Nonlinear magnetic force and dynamic characteristics of a tri-stable piezoelectric energy harvester”, *Nonlinear Dyn.*, **97**, 2371-2397. https://doi.org/10.1007/s11071-019-05133-z
Wang, G., Wu, H., Liao, W-H., Cui, S., Zhao, Z. and Tan, J. (2020), “A modified magnetic force model and experimental validation of a tri-stable piezoelectric energy harvester”, *J. Intell. Mater. Syst. Struct.*, **31**(7), 967-979. https://doi.org/10.1177/1045389X20905975
Wu, H., Tang, L., Yang, Y. and Soh, C.K. (2014), “Development of a broadband nonlinear two-degree-of-freedom piezoelectric energy harvester”, *J. Intell. Mater. Syst. Struct.*, **25**(14), 1875-1889. https://doi.org/10.1177/1045389X14541494
Yang, W. and Towfighian, S. (2017), “A hybrid nonlinear vibration energy harvester”, *Mech. Syst. Signal Process.*, **90**, 317-333. https://doi.org/10.1016/j.ymssp.2016.12.032
Zhou, S., Cao, J., Erturk, A. and Lin, J. (2013), “Enhanced broadband piezoelectric energy harvesting using rotatable magnets”, *Appl. Phys. Lett.*, **102**, Article 173901. https://doi.org/10.1063/1.4803445
Zou, H.X., Zhao, L.C., Gao, Q.H., Zuo, L., Liu, F.R., Tan, T., Wei, K.X. and Zhang, W.M. (2019), “Mechanical modulations for enhancing energy harvesting: Principles, methods and applications”, *Appl. Energy*, **255**, p. 113871. https://doi.org/10.1016/j.apenergy.2019.113871

FC